

# Thermoelectric properties of an ultra-thin topological insulator

SK Firoz Islam and Tarun Kanti Ghosh

*Department of Physics, Indian Institute of Technology-Kanpur, Kanpur-208 016, India*

(Dated: August 23, 2021)

Thermoelectric coefficients of an ultra-thin topological insulator are presented here. The hybridization between top and bottom surface states of a topological insulator plays a significant role. In absence of magnetic field, thermopower increases and thermal conductivity decreases with increase of the hybridization energy. In presence of magnetic field perpendicular to the ultra-thin topological insulator, thermoelectric coefficients exhibit quantum oscillations with inverse magnetic field, whose frequency is strongly modified by the Zeeman energy and phase factor is governed by the product of the Lande  $g$ -factor and the hybridization energy. In addition to the numerical results, the low-temperature approximate analytical results of the thermoelectric coefficients are also provided. It is also observed that for a given magnetic field these transport coefficients oscillate with hybridization energy, whose frequency depends on the Lande  $g$ -factor.

PACS numbers: 73.50.-h, 73.50.Lw,

## I. INTRODUCTION

Recently a new class of material, called topological insulator, has been paid much attention by condensed matter physicists<sup>1-6</sup>. Topological insulator (TI) shows the conduction of electrons on the surface of 3D materials otherwise behaves as an insulator. It is due to the time-reversal symmetry possessed by materials like  $\text{Bi}_2\text{Se}_3$ ,  $\text{Sb}_2\text{Te}_3$  and  $\text{Bi}_2\text{Te}_3$ <sup>6</sup>. The conducting surface states of these material show a single Dirac cone, in which spin is always locked perpendicular to it's momentum. The angle resolved photoemission spectroscopy<sup>7-9</sup> or scanning tunneling microscopy<sup>10</sup> has been used to realize the single Dirac cone in TIs. In two-dimensional electron systems, under the presence of a perpendicular magnetic field, electron conduction along the boundary due to the circular orbits bouncing off the edges, leading to skipping orbits. However, in 3D materials, even in absence of magnetic field electron conduction takes place on the surface. Here, strong Rashba spin-orbit coupling (RSOC) plays the role of magnetic field. The RSOC originates from the lack of structural inversion symmetry of the sample<sup>11,12</sup>.

Though there have been several experimental works on the surface states of TIs, one of the major obstacle in studying the transport properties of the surface is the unavoidable contribution of the bulk. One of the best method to minimize this problem is to grow TIs sample in the form of ultra-thin films, in which bulk contribution becomes relatively very small in comparison to the surface contribution<sup>13-15</sup>. The transition from 3D to 2D TIs lead to several effects which have been studied for different thickness<sup>15,16</sup>. The ultra-thin TI not only reduces the bulk contribution, but also possesses some new phenomenon like possible excitonic superfluidity<sup>17</sup>, unique magneto-optical response<sup>18-20</sup> and better thermoelectric performances<sup>21</sup>. Moreover, the small thickness leads to the overlap of the wave functions between top and bottom surfaces which introduces a new degree of

freedom hybridization<sup>22,23</sup>. However, it happens to a certain thickness of five to ten quintuple layers<sup>15,24</sup> i.e; of the order of 10 nm. The oscillating exponential decay of hybridization induced band gap with reducing thickness in  $\text{Bi}_2\text{Te}_3$  has been also reported theoretically<sup>25</sup>. The formation of Landau levels have been confirmed by several experiments<sup>26,27</sup> in thin TIs. Moreover, several theoretical study on low-temperature transport properties in a series of works<sup>24,28-31</sup> have been reported.

Thermoelectric properties of materials<sup>32</sup> have always been interesting topic for providing an additional way in exploring the details of an electronic system. When a temperature gradient is applied across the two ends of the electronic system, the migration of electrons from hotter to cooler side leads to the development of a voltage gradient across these ends. This voltage difference per unit temperature gradient is known as longitudinal thermopower. In addition to this temperature gradient if a perpendicular magnetic field is applied to the system, due to Lorentz force, a transverse electric field is also established and gives transverse thermopower. In conventional 2D electronic system, Landau levels induced quantum oscillation (Shubnikov-de Hass) in thermoelectric coefficients has been reported theoretically as well as experimentally in a series of works<sup>33-37</sup>. In 3D TIs, improvement of thermoelectric performance without magnetic field have been predicted theoretically in a series of paper<sup>38-41</sup>. In the newly emerged relativistic-like 2D electron system-graphene, thermoelectric effects have been also studied<sup>42-45</sup>.

In this paper, we study the effect of hybridization on the thermopower and the thermal conductivity of the ultra-thin TIs in absence/presence of magnetic field. We find thermopower increases and thermal conductivity decreases with increase of the hybridization energy when magnetic field is absent. In presence of perpendicular magnetic field, thermoelectric coefficients oscillate with inverse magnetic field. The frequency of the quantum oscillations is strongly modified by the Zeeman energy,

and phase factor is determined by the product of the Lande  $g$ -factor and the hybridization energy. The analytical expressions of the thermoelectric coefficients are also obtained. It is also shown that these transport coefficients oscillate with frequency depend on hybridization energy and Lande  $g$ -factor.

This paper has following structure. Section II briefly discusses energy spectrum and the density of states of the ultra-thin TI in absence and presence of magnetic field. In section III, we have studied how the hybridization affects the thermoelectric coefficients for zero magnetic field. In section IV, a complete analysis of thermoelectric coefficients in present of magnetic field is provided with numerical and analytical results. We provide a summary and conclusion of our work in section V.

## II. ENERGY SPECTRUM AND DENSITY OF STATES

### A. Zero magnetic field case

Let us consider a surface of an ultra-thin TI in  $xy$ -plane with  $L_x \times L_y$  dimension, and carriers are Dirac fermions occupying the top and bottom surfaces of the TI. The quantum tunneling between top and bottom surfaces gives rise to the hybridization and consequently the Hamiltonian can be written as the symmetric and anti-symmetric combination of both surface states as<sup>22</sup>

$$H = \begin{bmatrix} h(k) & 0 \\ 0 & h^*(k) \end{bmatrix}, \quad (1)$$

with  $h(k) = \Delta_h \sigma_z + v_F(p_y \sigma_x - p_x \sigma_y)$ . Here  $\mathbf{p}$  is the two-dimensional momentum operator,  $v_F$  is the Fermi velocity of the Dirac fermion,  $\boldsymbol{\sigma} = (\sigma_x, \sigma_y, \sigma_z)$  are the Pauli spin matrices and  $\Delta_h$  is the hybridization matrix element between the states of the top and bottom surfaces of the TI. Typical value of  $\Delta_h$  varies from  $(0 - 10^2)$  meV depending on the thickness of the 3D TI<sup>15</sup>. Because of the block-diagonal nature, the above Hamiltonian can be written as

$$H = v_F(\sigma_x p_y - \tau_z \sigma_y p_x) + \Delta_h \sigma_z, \quad (2)$$

where  $\tau_z = \pm$  denotes symmetric and anti-symmetric surface states, respectively. The energy spectrum of the Dirac electron is given by

$$E = \lambda \sqrt{(\hbar v_F k)^2 + \Delta_h^2}. \quad (3)$$

Here  $\lambda = \pm$  stands for electron and hole bands. The density of states is given by

$$D_0(E) = \frac{2E}{\pi \hbar^2 v_F^2}. \quad (4)$$

### B. Non-zero magnetic field case

In presence of magnetic field perpendicular to the surface, the Hamiltonian for Dirac electron with hybridization is

$$H = v_F(\sigma_x \Pi_y - \tau_z \sigma_y \Pi_x) + (\tau_z \Delta_z + \Delta_h) \sigma_z, \quad (5)$$

where  $\boldsymbol{\Pi} = \mathbf{p} + e\mathbf{A}$  is the two-dimensional canonical momentum operator. Using Landau gauge  $\vec{A} = (0, Bx, 0)$ , exact Landau levels can be obtained very easily<sup>28,31</sup>. For  $n = 0$ , there is only one energy level which is given as  $E_0^{\tau_z} = -(\Delta_z + \tau_z \Delta_h)$ . When integer  $n \geq 1$ , there are two energy bands denoted by  $+$  corresponding to the electron and  $-$  corresponding to the hole with energy

$$E_{n,\lambda}^{\tau_z} = \lambda \sqrt{2n(\hbar\omega_c)^2 + (\Delta_z + \tau_z \Delta_h)^2}, \quad (6)$$

where  $\omega_c = v_F/l$  is the cyclotron frequency with  $l = \sqrt{\hbar/(eB)}$  is the magnetic length,  $\Delta_z = g\mu_B B/2$  with  $g$  is the Lande  $g$ -factor.

The corresponding eigenstates for symmetric surface state are

$$\Psi_n^+(\mathbf{r}) = \frac{e^{ik_y y}}{\sqrt{L_y}} \begin{pmatrix} c_1 \phi_{n-1}(x+x_0) \\ c_2 \phi_n(x+x_0) \end{pmatrix}, \quad (7)$$

$$\Psi_n^-(\mathbf{r}) = \frac{e^{ik_y y}}{\sqrt{L_y}} \begin{pmatrix} c_2 \phi_{n-1}(x+x_0) \\ -c_1 \phi_n(x+x_0) \end{pmatrix}, \quad (8)$$

where  $\phi_n(x) = (1/\sqrt{\sqrt{\pi} 2^n n! l}) e^{-x^2/2l^2} H_n(x/l)$  is the normalized harmonic oscillator wave function,  $x_0 = -k_y l^2$ ,  $c_1 = \cos(\theta_{\tau_z}/2)$  and  $c_2 = \sin(\theta_{\tau_z}/2)$  with  $\theta_{\tau_z} = \tan^{-1}[\sqrt{n} \hbar \omega_c / (\Delta_z + \tau_z \Delta_h)]$ . The anti-symmetric surface state can be obtained by exchanging  $n$  and  $n-1$ .

We have derived approximate analytical form of density of states for  $n > 1$ , by using the Green's function technique which is given as (see Appendix A)

$$D_{\tau_z}(E) \simeq \frac{D_0(E)}{2} \left[ 1 + 2 \sum_{s=1}^{\infty} \exp \left\{ -s \left( 2\pi \frac{\Gamma_0 E}{\hbar^2 \omega_c^2} \right)^2 \right\} \right. \\ \left. \times \cos \left\{ \pi s \left( E^2 - \Delta_{\tau_z}^2 \right) / (\hbar \omega_c)^2 \right\} \right], \quad (9)$$

where  $\Delta_{\tau_z} = \Delta_z + \tau_z \Delta_h$  and  $\Gamma_0$  is the impurity induced Landau level broadening.

## III. THERMOELECTRIC COEFFICIENTS

In this section, we shall calculate thermoelectric coefficients of an ultra-thin TI in zero and non-zero magnetic fields.

### A. Zero-magnetic field case

In this sub-section, the effect of hybridization on thermopower and thermal conductivity is presented. We

follow most conventional approach at low temperature regime. The electrical current density  $\mathbf{J}$  and the thermal current density  $\mathbf{J}_q$  for Dirac electrons can be expressed under linear response regime as

$$\mathbf{J} = Q^{11}\mathbf{E} + Q^{12}(-\nabla T) \quad (10)$$

and

$$\mathbf{J}^q = Q^{21}\mathbf{E} + Q^{22}(-\nabla T), \quad (11)$$

where  $\mathbf{E}$  is the electric field,  $\nabla T$  is the temperature gradient and  $Q^{ij}$  ( $i, j = 1, 2$ ) are the phenomenological transport coefficients. The above equations describe the response of electronic system under the combined effects of thermal and potential gradient. Moreover,  $Q^{ij}$  can be expressed in terms of an integral  $I^{(r)}$ :  $Q^{11} = I^{(0)}$ ,  $Q^{21} = TQ^{12} = -I^{(1)}/e$ ,  $Q^{22} = I^{(2)}/(e^2T)$  with

$$I^{(r)} = \int dE \left[ -\frac{\partial f(E)}{\partial E} \right] (E - \eta)^{(r)} \sigma(E), \quad (12)$$

where  $r = 0, 1, 2$  and  $f(E) = 1/[1 + \exp(E - \eta)\beta]$  is the Fermi-Dirac distribution function with  $\eta$  is the chemical potential and  $\beta = (k_B T)^{-1}$ . Here,  $\sigma(E)$  is the energy-dependent electrical conductivity. When circuit is open i.e; for  $J = 0$ , thermopower can be defined as  $S = Q^{12}/Q^{11}$ . By using Sommerfeld expansion at low temperature regime, diffusive thermopower  $S$  and thermal conductivity  $\kappa$  can be obtained from Mott's relation and the Wiedemann-Franz law as

$$S = -L_0 e T \left[ \frac{d}{dE} \ln \sigma(E) \right]_{E=E_F} \quad (13)$$

and

$$\kappa = L_0 T \sigma(E_F). \quad (14)$$

Here,  $L_0 = (\pi^2 k_B^2)/(3e^2) = 2.44 \times 10^{-8} \text{ W}\Omega\text{K}^{-2}$  is the Lorentz number and  $\sigma(E_F)$  is the electrical conductivity at the Fermi energy.

Classical Boltzmann transport equation can be used to calculate zero magnetic field electrical conductivity, which is given by<sup>49</sup>

$$\sigma_{ij}(E) = e^2 \tau(E) \int \frac{d^2 k}{(2\pi)^2} \delta[E - E(k)] v^i(k) v^j(k), \quad (15)$$

where  $i, j = x, y$ . For isotropic system  $v_x^2 = v_y^2 = (1/2)(v_x^2 + v_y^2) = (1/2)v^2$ . In our case,

$$v^2 = \frac{v_F^2}{2} \left[ 1 - \left( \frac{\Delta_h}{E} \right)^2 \right]. \quad (16)$$

Using these in Eq.[15], the energy dependent conductivity becomes as

$$\sigma(E) = e^2 \tau(E) \frac{E}{\pi \hbar^2} \left[ 1 - \left( \frac{\Delta_h}{E} \right)^2 \right]. \quad (17)$$

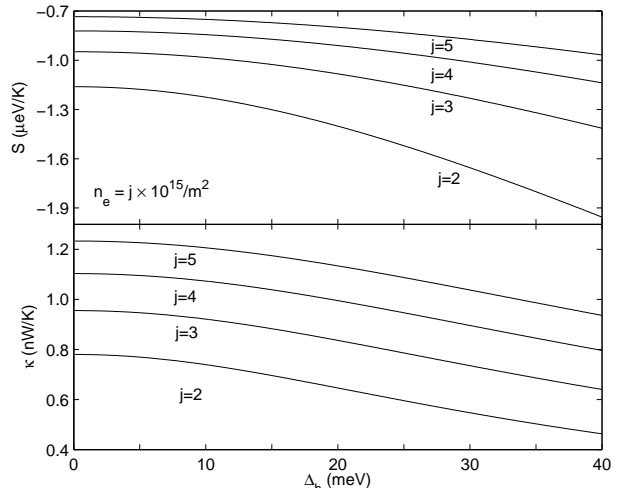


FIG. 1. Plots of the thermopower versus hybridization constant for  $m = 1$  and for various carrier density.

Assuming the energy dependent scattering time to be  $\tau = \tau_0 (E/E_F)^m$ , where  $m$  is a constant depending on the scattering mechanism,  $E_F = \sqrt{E_{F0}^2 + \Delta_h^2}$  is the Fermi energy with  $E_{F0} = \hbar v_F k_F^0$ . Here, Fermi vector  $k_F^0 = \sqrt{2\pi n_e}$ . Substituting Eq. (17) into Eq. (13), the diffusion thermopower is obtained as

$$S = -L_0 \frac{eT}{E_{F0}} \left[ (m+1) + 2 \left( \frac{\Delta_h}{E_{F0}} \right)^2 \right] / \sqrt{1 + \left( \frac{\Delta_h}{E_{F0}} \right)^2}. \quad (18)$$

We plot thermopower versus hybridization for different carrier density in the upper panel of Fig. [1]. It shows that thermopower increases with increasing hybridization for a particular carrier density. But for higher carrier density, this rate of enhancement with hybridization becomes very slow.

Thermal conductivity can be directly obtained from Wiedemann-Franz law given in Eq. (14) where the electrical conductivity  $\sigma(E_F)$  is given as

$$\sigma = \sigma_0 / \sqrt{1 + \left( \frac{\Delta_h}{E_{F0}} \right)^2}. \quad (19)$$

Here,  $\sigma_0 = e^2 \tau_0 E_{F0} / (\pi \hbar^2)$  is the Drude conductivity without the hybridization constant for the Dirac system. Thermal conductivity is plotted in the the lower panel of Fig. [1]. We note that the thermal conductivity is diminished with increasing hybridization. However, unlike the case of thermopower, here thermal conductivity increases with carrier density.

## B. Non-zero magnetic field case

In presence of magnetic field, the classical approach can not explain the phenomenon depend on energy quan-

tization. In this sub-section we follow quantum mechanical approach, based on linear response theory, to study thermal transport coefficients. Thermoelectric coefficients for two-dimensional electron system in presence of magnetic field were derived by modifying the Kubo formula in Ref.<sup>46,47</sup>. These phenomenological transport coefficients are

$$\sigma_{\mu\nu} = \mathcal{L}_{\mu\nu}^{(0)} \quad (20)$$

$$S_{\mu\nu} = \frac{1}{eT} [(\mathcal{L}^{(0)})^{-1} \mathcal{L}^{(1)}]_{\mu\nu} \quad (21)$$

$$\kappa_{\mu\nu} = \frac{1}{e^2 T} [\mathcal{L}_{\mu\nu}^{(2)} - eT(\mathcal{L}^{(1)} S)_{\mu\nu}], \quad (22)$$

where

$$\mathcal{L}_{\mu\nu}^{(r)} = \int dE \left[ -\frac{\partial f(E)}{\partial E} \right] (E - \eta)^r \sigma_{\mu\nu}(E). \quad (23)$$

Here,  $\mu, \nu = x, y$ . Also,  $\sigma_{\mu\nu}(E)$ ,  $S_{\mu\nu}$  and  $\kappa_{\mu\nu}$  are the zero-temperature energy-dependent conductivity, thermopower and thermal conductivity tensors, respectively.

Generally, diffusive and collisional mechanism play major role in electron conduction. The quantized energy spectrum of electrons results itself through Shubnikov-de Hass oscillation by collisional mechanism. In our case, electron transport is mainly due to the collisional instead of diffusive. The zero drift velocity of electron do not allow to have diffusive contribution. In presence of temperature gradient, thermal transport coefficients can be expressed as  $\mathcal{L}_{xx}^{(r)} = \mathcal{L}_{xx}^{(r)\text{col}} = \mathcal{L}_{yy}^{(r)\text{col}}$  and  $\mathcal{L}_{yy}^{(r)} = \mathcal{L}_{yy}^{(r)\text{dif}} + \mathcal{L}_{yy}^{(r)\text{col}} = \mathcal{L}_{yy}^{(r)\text{col}}$ . In Ref.<sup>31</sup>, the exact form of the finite temperature collisional conductivity has been calculated for the screened impurity potential  $U(\mathbf{k}) = 2\pi e^2 / (\epsilon \sqrt{k^2 + k_s^2}) \simeq 2\pi e^2 / (\epsilon k_s) = U_0$  under the limit of small  $|\mathbf{k}| \ll k_s$  with  $k_s$  and  $\epsilon$  being the inverse screening length and dielectric constant of the material, respectively. In this limit, one can use  $\tau_0^2 \approx \pi l^2 \hbar^2 / N_I U_0^2$  with  $\tau_0$  is the relaxation time,  $U_0$  is the strength of the screened impurity potential and  $N_I$  is the two-dimensional impurity density. The exact form of the finite temperature conductivity<sup>31</sup> can be reduced to the zero-temperature energy-dependent electrical conductivity as

$$\sigma_{xx}(E) = \frac{e^2}{h} \frac{N_I U_0^2}{\pi \Gamma_0 l^2} \sum_{\tau_z} I_n^{\tau_z}, \quad (24)$$

where  $I_n^{\tau_z} = [n\{1 + \cos^2(\theta_{\tau_z})\} - \cos(\theta_{\tau_z})]$ . Here we have used  $-\partial f/\partial E = \delta[E - E_n^{\tau_z}]$ . Using Eq. (23), the finite temperature diagonal ( $\mathcal{L}_{xx}^{(r)}$ ) and off-diagonal coefficients ( $\mathcal{L}_{yx}^{(r)}$ ) can be written as

$$\mathcal{L}_{xx}^{(r)} = \frac{e^2}{h} \frac{N_I U_0^2}{\pi \Gamma_0 l^2} \sum_{n, \tau_z} I_n^{\tau_z} \left[ (E - \eta)^r \left( -\frac{\partial f(E)}{\partial E} \right) \right]_{E=E_n^{\tau_z}} \quad (25)$$

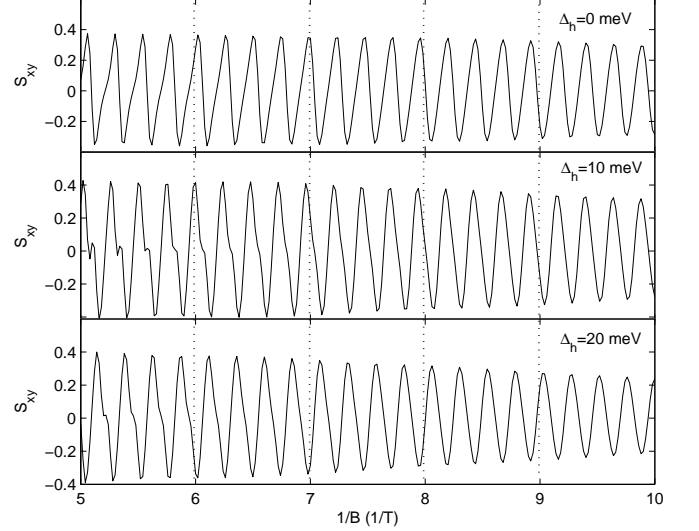


FIG. 2. Plots of the thermopower in units of  $k_B/e$  versus inverse magnetic field for different values of the hybridization constant.

and

$$\mathcal{L}_{yx}^{(r)} = \frac{e^2}{h} \frac{1}{2} \sum_{n, \tau_z} \frac{\sin^2 \theta_{\tau_z}}{\Delta_n^2} \int_{E_n, \tau_z}^{E_{n+1}, \tau_z} (E - \eta)^r \left( -\frac{\partial f(E)}{\partial E} \right) dE. \quad (26)$$

Here,  $\Delta_n = \sqrt{2n + (\frac{\Delta_{\tau_z}}{\hbar \omega_c})^2} - \sqrt{2(n+1) + (\frac{\Delta_{\tau_z}}{\hbar \omega_c})^2}$ .

#### IV. NUMERICAL RESULTS AND DISCUSSION

In our numerical calculations, the following parameters are used: carrier concentration  $n_e = 2 \times 10^{15} \text{ m}^{-2}$ ,  $g = 60$ ,  $v_F = 4 \times 10^5 \text{ m s}^{-1}$  and  $T = 0.7 \text{ K}$ . These numerical parameters are consistent with Ref.<sup>15,30,31</sup>.

In Fig. [2], the off-diagonal thermopower,  $S_{xy}$ , as a function of the inverse magnetic field for different values of the hybridization constant is shown. Similarly, the thermal conductivity,  $\kappa_{xx}$ , versus inverse magnetic field for different values of the hybridization constant is shown in Fig. [3]. Careful observation of these two figures clearly show that both  $S_{xy}$  and  $\kappa_{xx}$  oscillate with the same frequency which does not depend on the hybridization energy. The hybridization energy only influences the phase of oscillations.

To determine the frequency and the phase of the quantum oscillations in the thermoelectric coefficients, we shall derive analytical expressions of these coefficients. The components of the thermopower are given by

$$S_{xx} = S_{yy} = \frac{1}{eT} \left[ \frac{\sigma_{xx}}{S_0} \mathcal{L}_{xx}^{(1)} + \frac{\mathcal{L}_{yx}^{(1)}}{\sigma_{yx}} \right] \quad (27)$$

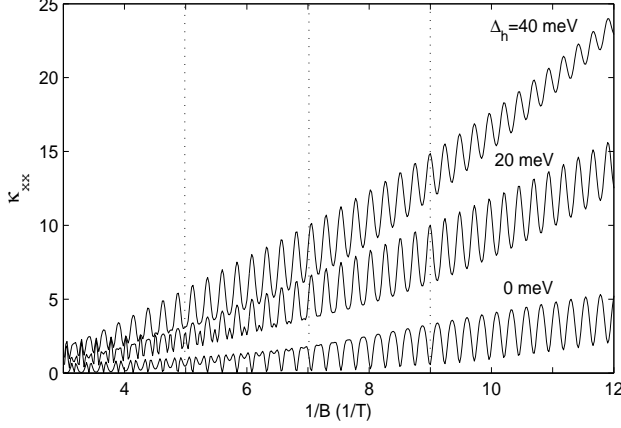


FIG. 3. Plots of the thermal conductivity in units of  $k_B^2/h$  versus inverse magnetic field.

and

$$S_{xy} = -S_{yx} = \frac{1}{eT} \left[ \frac{\sigma_{xx}}{S_0} (-\mathcal{L}_{xy}^{(1)}) + \frac{\mathcal{L}_{xx}^{(1)}}{\sigma_{yx}} \right]. \quad (28)$$

Here,  $S_0 = \sigma_{xx}\sigma_{yy} - \sigma_{xy}\sigma_{yx}$ . The dominating term in the above two equations is the last term. The analytical form of  $\kappa_{xx}$  and  $S_{xy}$  can be obtained directly by deriving analytical form of the phenomenological transport coefficients. The analytical form of density of states given in Eq. (9) allows us to obtain asymptotic expressions of  $S_{xy}$  and  $\kappa_{xx}$ . This is done by replacing the summation over discrete quantum numbers  $n$  by the integration i.e;  $\sum_n \rightarrow 2\pi l^2 \int D_{\tau_z}(E) dE$ , then we get

$$\mathcal{L}_{xx}^{(1)} \simeq \frac{4\pi e^2}{\beta} \frac{\Gamma_0 E_F}{h (\hbar\omega_c)^2} \Omega_D G'(x) \sum_{\tau_z} U_{\tau_z} F_{\tau_z} \sin(2\pi F_{\tau_z}) \quad (29)$$

and

$$\mathcal{L}_{xx}^{(2)} \simeq \frac{L_0 e^2 T^2 \sigma_0}{(\omega_c \tau_0)^2} \sum_{\tau_z} U_{\tau_z} F_{\tau_z} [1 - 3\Omega_D G''(x) \cos(2\pi F_{\tau_z})], \quad (30)$$

where  $F_{\tau_z} = (E_F^2 - \Delta_{\tau_z}^2)/(\sqrt{2}\hbar\omega_c)^2$ ,  $U_{\tau_z} = [1 + \cos^2(\bar{\theta}_{\tau_z})]$ , the impurity induced damping factor is

$$\Omega_D = \exp \left\{ - \left( 2\pi \frac{\Gamma_0 E_F}{\hbar^2 \omega_c^2} \right)^2 \right\} \quad (31)$$

and the temperature dependent damping factor is the derivative of the function  $G(x)$  with  $G(x) = x/\sinh(x)$ . Here,  $x = T/T_c$  with  $T_c = (\hbar\omega_c)^2/(2\pi^2 k_B E_F)$  is the critical temperature which depends on strength of hybridization through Fermi energy. Note that  $G(x)$  is the temperature dependent damping factor for the electrical conductivity tensor.

The off-diagonal thermopower  $S_{xy}$  and the diagonal

thermal conductivity  $\kappa_{xx}$  are obtained as given by

$$S_{xy} \simeq \frac{k_B}{e} \frac{1}{k_F^0 l} \frac{16\pi}{\omega_c \tau_0} \left[ 1 + \left( \frac{\Delta_h}{E_{F0}} \right)^2 \right]^{1/2} \Omega_D G'(x) \times \sum_{\tau_z} \frac{U_{\tau_z}}{\sin^2(\bar{\theta}_{\tau_z})} F_{\tau_z} \sin(2\pi f/B - \tau_z \phi) \quad (32)$$

and

$$\kappa_{xx} \simeq L_0 \frac{\sigma_0 T}{(\omega_c \tau_0)^2} \sum_{\tau_z} U_{\tau_z} F_{\tau_z} \times \left[ 1 - 6\Omega_D G''(x) \cos(2\pi f/B - \tau_z \phi) \right], \quad (33)$$

where the frequency  $f$  is given as

$$f = \frac{1}{2e\hbar v_F^2} (E_{F0}^2 - \Delta_z^2) \quad (34)$$

and the phase factor  $\phi = \pi g \mu_B \Delta_h / (e\hbar v_F^2)$ . Therefore, the thermopower and the thermal conductivity oscillate with the same frequency  $f$  which is independent of  $\Delta_h$ , which can be shown from numerical result also. The oscillation frequency is strongly reduced by the Zeeman energy  $\Delta_z$ . On the other hand, the phase factor  $\phi$  is related to the product of the Lande  $g$ -factor and  $\Delta_h$  and it vanishes if either of them is zero. Although the frequency and the phase of  $S_{xx}$  and  $\kappa_{xx}$  are the same but the damping factor and amplitude are different.

Now we compare the numerical and analytical results of  $S_{xy}$  and  $\kappa_{xx}$  in Fig. [4]. For better visualization, we have taken weak Landau level broadening  $\Gamma_0 = 0.01$  meV for  $S_{xy}$  and  $\kappa_{xx}$ . The analytical results, in particular the frequency  $f$ , match very well with the numerical results. We must mention here that for different values of  $\Gamma_0$  analytical results may differ with numerical in the amplitude but the frequency and phase are always in good agreement.

It is interesting to see from the analytical expressions of the thermopower and the thermal conductivity that these transport coefficients possess weak periodic oscillation with the hybridization energy for a given magnetic field. These oscillation is shown in figure 5.. The frequency and phase factor of these oscillations for a fixed  $B$  are  $\nu = \phi/(2\pi) = g\mu_B/(2e\hbar v_F^2)$  and  $\Phi = 2\pi f/B$ , respectively.

In presence of the magnetic field, these approximate analytical expression of the thermopower and thermal conductivity can be also used for monolayer graphene by putting  $\Delta_h = 0$ . There are several experimental results<sup>42,48</sup> on thermoelectric properties of a graphene monolayer but analytical expressions are not available in the literature. The approximate analytical expression of the thermopower and thermal conductivity can also be used for a monolayer graphene by setting  $\Delta_h = 0$ .

## V. CONCLUSION

We have presented a theoretical study on the thermoelectric coefficients of ultra-thin topological insulators in

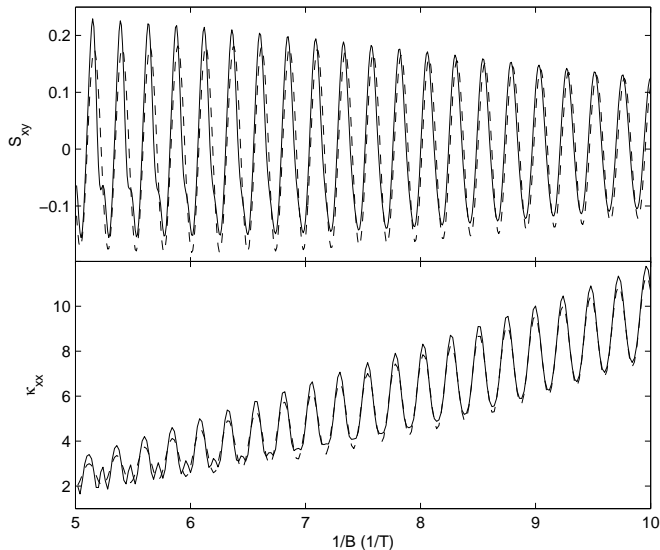


FIG. 4. Plots of the numerical and analytical results of the thermoelectric coefficients versus inverse magnetic field for  $\Delta_h = 20$  meV. Solid and dashed lines stand for numerical and analytical results, respectively.

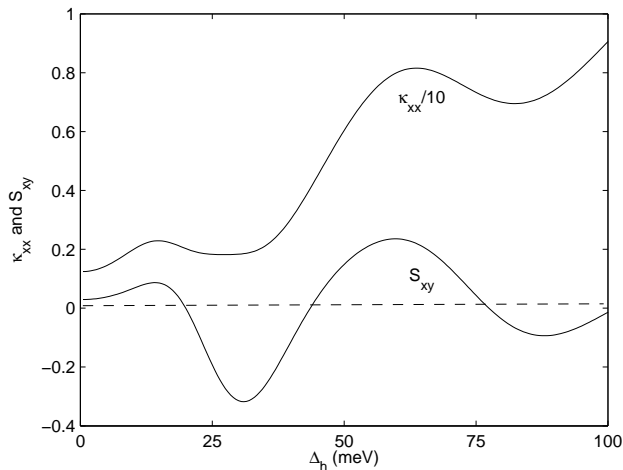


FIG. 5. Plots of the thermopower and thermal conductivity versus the hybridization constant ( $\Delta_h$ ). Here,  $B = 0.2$  T is taken.

presence/absence of the magnetic field. In absence of the magnetic field, the thermopower and the thermal conductivity are modified due to the hybridization between top and bottom surface states. The thermopower is enhanced and the thermal conductivity is diminished due to the hybridization. The quantum oscillations in the thermopower and the thermal conductivity for different values of the hybridization constant are also studied numerically. In addition to the numerical results, we ob-

tained the analytical expressions the thermopower ( $S_{xy}$ ) and the thermal conductivity ( $\kappa_{xx}$ ). The analytical results match very well with the numerical results. We have also provided analytical expressions of the oscillation frequency and phase. The oscillation frequency is the same for both the thermopower and thermal conductivity. It is independent of the hybridization constant but strongly suppressed by the Zeeman energy. On the other hand, the hybridization constant plays a very significant role in the phase as well as in the amplitude of the oscillations. From the analytical results, critical temperature ( $T_c$ ) is found to be reduced with increasing hybridization constant. Thermoelectric coefficients also show a very low-frequency oscillation with the hybridization constant for a given magnetic field. Moreover, our analytical expressions of the thermopower and thermal conductivity are also applicable for a graphene monolayer by setting  $\Delta_h = 0$ .

## VI. ACKNOWLEDGEMENT

This work is financially supported by the CSIR, Govt. of India under the grant CSIR-SRF-09/092(0687) 2009/EMR F-O746.

## Appendix A

Derivation of asymptotic analytical expression of density of states of a two dimensional electronic system in presence of impurity can be done by calculating self-energy<sup>50,51</sup> which is given as

$$\Sigma^-(E) = \Gamma_0^2 \sum_n \frac{1}{E - E_n^{\tau_z} - \Sigma^-(E)}. \quad (\text{A1})$$

Imaginary part of the self-energy is related to density of states as  $D(E) = \text{Im} \left[ \frac{\Sigma^-(E)}{\pi^2 I^2 \Gamma_0^2} \right]$ .

By using residue theorem, we calculate the summation in Eq.(A1), which give  $\Sigma^-(E) \simeq \frac{2\pi\Gamma_0^2 E}{(\hbar\omega_c)^2} \cot(\pi n_0)$ , where  $n_0$  is the pole and given as

$$n_0 = \frac{1}{2(\hbar\omega_c)^2} \left[ \{E - \Sigma^-(E)\}^2 - (\Delta_z + \tau_z \Delta_h)^2 \right]. \quad (\text{A2})$$

By writing the self-energy as the sum of real and imaginary part, it can be further simplified as

$$\Delta + i\frac{\Gamma}{2} \simeq \frac{2\pi\Gamma_0^2 E}{(\hbar\omega_c)^2} \cot \left[ \frac{(u - iv)}{2} \right] \quad (\text{A3})$$

Here,

$$u = \frac{\pi}{(\hbar\omega_c)^2} [E^2 - (\Delta_z + \tau_z \Delta_h)^2] \quad (\text{A4})$$

and  $v = \pi\Gamma E/(\hbar\omega_c)^2$ . The imaginary part is  $\frac{\Gamma}{2} = \frac{2\pi\Gamma_0^2 E}{(\hbar\omega_c)^2} \frac{\sinh v}{\cosh v - \cos u}$ . Now, this can be re-written by using the following standard relation as

$$\frac{\sinh v}{\cosh v - \cos u} = 1 + 2 \sum_{s=1}^{\infty} e^{-sv} \cos(su). \quad (\text{A5})$$

Here, the most dominant term is for  $s = 1$  only. We can write

$$\frac{\Gamma}{2} = \frac{2\pi\Gamma_0^2 E}{(\hbar\omega_c)^2} \left[ 1 + 2 \sum_{s=1}^{\infty} e^{-s\pi\Gamma E/(\hbar\omega_c)^2} \cos(su) \right]. \quad (\text{A6})$$

In the limit of  $\pi\Gamma \gg \hbar\omega_c$ , after first iteration, we have  $\Gamma/2 = 2\pi\Gamma_0^2 E/(\hbar\omega_c)^2$ . Substituting it in the earlier expression, we get

$$\frac{\Gamma}{2} = \frac{2\pi\Gamma_0^2 E}{(\hbar\omega_c)^2} \left[ 1 + 2 \sum_{s=1}^{\infty} \exp \left\{ -s \left( \frac{2\pi\Gamma_0 E}{\hbar^2 \omega_c^2} \right)^2 \right\} \cos \left\{ s\pi \left( E^2 - \Delta_{\tau_z}^2 \right) / (\hbar\omega_c)^2 \right\} \right]. \quad (\text{A7})$$

Here,  $\Delta_{\tau_z} = \Delta_z + \tau_z \Delta_h$

Finally, the density of states for two branches can be obtained as

$$D_{\tau_z}(E) = \frac{D_0(E)}{2} \left[ 1 + 2 \sum_{s=1}^{\infty} \exp \left\{ -s \left( \frac{2\pi\Gamma_0 E}{\hbar^2 \omega_c^2} \right)^2 \right\} \cos \left\{ s\pi \left( E^2 - \Delta_{\tau_z}^2 \right) / (\hbar\omega_c)^2 \right\} \right]. \quad (\text{A8})$$

- 
- <sup>1</sup> C. L. Kane and E. J. Mele, Phys. Rev. Lett. **95**, 146802 (2005)
- <sup>2</sup> B. A. Bernevig, T. L. Hughes, and S. C. Zhang, Science **314**, 1757 (2006)
- <sup>3</sup> M. König, S. Wiedmann, C. Brune, A. Roth, H. Buhmann, L. W. Molenkamp, X. L. Qi, and S. C. Zhang, Science **318**, 766 (2007)
- <sup>4</sup> J. E. Moore and L. Balents, Phys. Rev. B **75**, 121306 (2007)
- <sup>5</sup> L. Fu, C. L. Kane, and E. J. Mele, Phys. Rev. Lett. **98**, 106803 (2007)
- <sup>6</sup> M. Zhang, C. X. Liu, X. L. Qi, X. Dai, Z. Fang, and S. C. Zhang, Nat. Phys. **5**, 438 (2009)
- <sup>7</sup> D. Hsieh, D. Qian, L. Wray, Y. Xia, Y. S. Hor, R. J. Cava, and M. Z. Hasan, Nature **452**, 970 (2008)
- <sup>8</sup> D. Hsieh, Y. Xia, L. Wray, D. Qian, A. Pal, J. H. Dil, J. Osterwalder, F. Meier, G. Bihlmayer, C. L. Kane, Y. S. Hor, R. J. Cava, and M. Z. Hasan, Science **323**, 919 (2009)
- <sup>9</sup> Y. Xia, D. Qian, D. Hsieh, L. Wray, A. Pal, H. Lin, A. Bansil, D. Grauer, Y. S. Hor, R. J. Cava, and M. Z. Hasan, Nat. Phys. **5**, 398 (2009)
- <sup>10</sup> P. Roushan, J. Seo, C. V. Parker, Y. S. Hor, D. Hsieh, D. Qian, A. Richardella, M. Z. Hasan, R. J. Cava, and A. Yazdani, Nature **460**, 1106 (2009)
- <sup>11</sup> E. I. Rashba and V. I. Sheka, Fizika Tverdogo Tela; Collected Papers vol 2 (Moscow and Leningrad: Academy of Sciences of the USSR) 162 (1959); E. I. Rashba, Sov. Phys.-Solid State 2, 1109 (1960)
- <sup>12</sup> Y. A. Bychkov and E. I. Rashba, J. Phys. C: Solid State, **17**, 6039 (1984)
- <sup>13</sup> G. Zhang, H. Qin, J. Teng, J. Guo, Q. Guo, X. Dai, Z. Fang, and K. Wu, Appl. Phys. Lett. **95**, 053114 (2009)
- <sup>14</sup> H. Peng, K. Lai, D. Kong, S. Meister, Y. Chen, X. L. Qi, S. C. Zhang, Z. X. Shen, and Y. Cui, Nat. Mater. **9**, 225 (2010)
- <sup>15</sup> Y. Zhang, K. He, C. Z. Chang, C. L. Song, L. L. Wang, X. Chen, J. F. Jia, Z. Fang, X. Dai, W. Y. Shan, S. Q. Shen, Q. Niu, X. L. Qi, S. C. Zhang, X. C. Ma, and Q. K. Xue, Nat. Phys. **6**, 584 (2010)
- <sup>16</sup> C. X. Liu, H. Zhang, B. Yan, X. L. Qi, T. Frauenheim, X. Dai, Z. Fang, and S. C. Zhang, Phys. Rev. B **81**, 041307 (2010)
- <sup>17</sup> B. Seradjeh, J. E. Moore, and M. Franz, Phys. Rev. Lett. **103**, 066402 (2010)
- <sup>18</sup> W. K. Tse and A. H. MacDonald, Phys. Rev. Lett. **105**, 057401 (2010)
- <sup>19</sup> W. K. Tse and A. H. MacDonald, Phys. Rev. B **82**, 161104 (2010)
- <sup>20</sup> J. Maciejko, X. L. Qi, and S. C. Zhang, Phys. Rev. Lett. **104**, 166803 (2010)
- <sup>21</sup> P. Ghaemi, R. S. K. Mong, and J. E. Moore, Phys. Rev. Lett. **105**, 166603 (2010)
- <sup>22</sup> R. Yu, W. Zhang, H. J. Zhang, S. C. Zhang, X. Dai, and Z. Fang, Science **329**, 61 (2010)
- <sup>23</sup> H. Z. Lu, W. Y. Shan, W. Yao, Q. Niu, S. Q. Shen, Phys. Rev. B **81**, 115407 (2010)
- <sup>24</sup> H. Cao, J. Tian, I. Miotkowski, T. Shen, J. Hu, S. Qiao, and Y. P. Chen, Phys. Rev. Lett. **108**, 216803 (2012)
- <sup>25</sup> J. Linder, T. Yokoyama, and A. Sudbo, Phys. Rev. B **80**, 205401 (2009)
- <sup>26</sup> P. Cheng, C. Song, T. Zhang, Y. Zhang, Y. Wang, J. F. Jia, J. Wang, Y. Wang, B. F. Zhu, X. Chen, X. Ma, K. He, L. Wang, X. Dai, Z. Fang, X. Xie, X. L. Qi, C. X. Liu, S. C. Zhang, and Q. K. Xue, Phys. Rev. Lett. **105**, 076801 (2010)
- <sup>27</sup> Y. Jiang, Y. Wang, M. Chen, Z. Li, C. Song, K. He, L. Wang, X. Chen, X. Ma, and Q. K. Xue, Phys. Rev. Lett. **108**, 016401 (2012)
- <sup>28</sup> A. A. Zyuzin, A. A. Barkov, Phys. Rev. B **83**, 195413 (2011)
- <sup>29</sup> J. Wang, A. M. DaSilva, C. Z. Chang, K. H., J. K. Jain, N. Samarth, X. C. Ma, Q. K. Xue, and M. H. W. Chan,

- Phys. Rev. B **83**, 245438 (2011)
- <sup>30</sup> M. Tahir, K. Sabeeh and U. Schwingenschlogl, Scientific Reports **3**, 1261 (2013)
- <sup>31</sup> M. Tahir, K. Sabeeh, and U. Schwingenschlogl, J. Appl. Phys. **113**, 043720 (2013)
- <sup>32</sup> G. S. Nolas, J. Sharp, and H. J. Goldsmid, *Thermoelectrics* (Springer-Verlag, Berlin, 2001)
- <sup>33</sup> R. Fletcher, J. C. Maan, K. Ploog, and G. Weimann, Phys. Rev. B **33**, 7122 (1986)
- <sup>34</sup> R. Fletcher, P. T. Coleridge, and Y. Feng, Phys. Rev. B **52**, 2823 (1995)
- <sup>35</sup> R. Fletcher, Semicond. Sci. Technol. **14**, R1 (1999)
- <sup>36</sup> S. Maximov, M. Gbordzoe, H. Buhmann, L. W. Molenkamp, and D. Reuter, Phys. Rev. B **70**, 121308 (R) (2004)
- <sup>37</sup> S. Goswami, C. Siegert, M. Pepper, I. Farrer, D. A. Ritchie, and A. Ghosh, Phys. Rev. B **83**, 073302 (2011)
- <sup>38</sup> O. A. Tretiakov, Ar. Abanov, S. Murakami, and J. Sinova, Appl. Phys. Lett. **97**, 073108 (2010)
- <sup>39</sup> O. A. Tretiakov, Ar. Abanov, and J. Sinova, Appl. Phys. Lett. **99**, 113110 (2011)
- <sup>40</sup> O. A. Tretiakov, Ar. Abanov, and J. Sinova, J. Appl. Phys. **111**, 07E319 (2012)
- <sup>41</sup> R. Takahashi and S. Murakami, Semicond. Sci. Technol. **27**, 124005 (2012)
- <sup>42</sup> Y. M. Zuev, W. Chang, and P. Kim, Phys. Rev. Lett. **102**, 096807 (2009)
- <sup>43</sup> P. Wei, W. Bao, Y. Pu, C. N. Lau, and J. Shi, Phys. Rev. Lett. **102**, 166808 (2009)
- <sup>44</sup> E. H. Hwang, E. Rossi, and S. Das Sarma, Phys. Rev. **B80**, 235415 (2009)
- <sup>45</sup> A. A. Patel and S. Mukerjee, Phys. Rev. B **86**, 075411 (2012)
- <sup>46</sup> L. Smreka and P. Streda, J. Phys. C: Solid State Phys. **10**, 2153 (1977)
- <sup>47</sup> H. Oji, J. Phys. C: Solid State Phys., **17**, 3059 (1984)
- <sup>48</sup> P. Wei, W. Bao, Y. Pu, C. N. Lau, and J. Shi, Phys. Rev. Lett. **102**, 166808 (2009)
- <sup>49</sup> N. W. Ashcroft and N. D. Mermin, Solid stste Physics, Cengage Learning (2010)
- <sup>50</sup> T. Ando, A. B. Fowler, and F. Stern, Rev. Mod. Phys. **54**, 437 (1982)
- <sup>51</sup> C. Zhang and R. R. Gerhardts, Phys. Rev. B **41**, 12850 (1990)